MONTE CARLO RESULTS FOR THE HADRON SPECTRUM

Richard Kenway

Department of Physics & Astronomy,
The University of Edinburgh,
The King's Buildings,
Edinburgh EH9 3JZ, Scotland.

INTRODUCTION

In these lectures, I will try to explain the important part played by hadron spectrum calculations in developing a reliable and quantitative numerical calculation scheme from first principles for QCD.

Why Calculate What is Well-Known?

The successful calculation of the spectrum of light hadrons, composed of u, d and s quarks, would, first of all, demonstrate that QCD correctly describes quark confinement at low energies. It would validate Monte Carlo simulation of QCD as a quantitative phenomenological tool, and this is vital, because many Standard Model parameters are obscured by non-perturbative QCD effects. Finally, computing the hadron spectrum would provide the most direct determination of the light quark masses, which are some of the most poorly-known Standard Model parameters.

Simply because we have to fix the quark masses before we can do anything else in QCD, spectrum calculations are the starting point for every simulation. Any error in the hadron mass estimates propagates through the calculation, to affect all predictions to some extent. So accuracy is crucial.

A Brief History

The first calculation was reported in 1981 by Hamber and Parisi[1], using a 6^3 spatial lattice and a computer with a speed of about 1 Mflops. They employed the quenched approximation, which neglects virtual quark-antiquark pairs, and Wilson quarks at $\beta = 6.0$ (see later), and they obtained reasonable agreement with experiment:

$$M_\rho = 800 \pm 100 \text{ MeV} \tag{1}$$

$$M_N = 950 \pm 100 \text{ MeV}. \tag{2}$$

However, their estimate of the scale (inverse lattice spacing), $a^{-1} = 1120$ MeV, is wrong by a factor two, most likely because of huge finite-size effects on such a small lattice. So the agreement with experiment was fortuitous! Nevertheless, their work showed that the low-energy properties of QCD were amenable to numerical simulation.

Subsequent progress may appear to have been slow. This is because it has largely entailed the controlling of systematic approximations, rather than any dramatic discoveries – after all, Hamber and Parisi *did agree* with experiment – and this has depended on significant progress in algorithms and machines. Nevertheless, I believe that no other area of computational science can match the rigour and sophistication that has been brought to bear on the calculation of the hadron masses.

In 1993, this topic hit the headlines with the announcement by the GF11 Collaboration that they had computed the hadron spectrum and found results within 6%, and 1.6 standard deviations, of the experimental values[2], using a purpose-built computer five thousand times faster than the one Hamber and Parisi had used. Remarkably, this claim was based on quenched simulations, not full QCD.

Today, following further progress in controlling lattice-spacing errors, the calculations are becoming accurate enough to show that the quenched results do disagree with experiment[3, 4] as, of course, they must!

HADRONS FROM LATTICE QCD

The spectrum, as well as many useful matrix elements, may be obtained from hadron correlation functions in Euclidean spacetime. The corresponding path integral is defined on a hypercubic lattice, in the limit of zero lattice spacing, $a \to 0$ in physical units. This limit occurs at a critical point of the lattice theory and the methods of statistical physics, Monte Carlo simulation and the renormalisation group, provide a tractable non-perturbative scheme for precise calculations[5].

The Lattice Formulation of QCD

Wilson Lattice Action. At every site, x, of the 4-dimensional lattice is a quark and antiquark field, $q(x)$ and $\bar{q}(x)$, which carry Dirac, colour and flavour indices. Associated with every link, (x, μ), of the lattice, from x to $x + a\hat{\mu}$, $\mu = 0, 1, 2, 3$, is a gauge field $U_\mu(x) \in SU(3)$. The Wilson lattice action[6] is

$$S[U, \bar{q}, q] = S_G[U] + S_F[U, \bar{q}, q]. \tag{3}$$

The gauge action is

$$S_G[U] = \frac{6}{g^2} \sum_{\Box} \Big[1 - \frac{1}{3} \mathrm{Re\ Tr}\ U_\Box\Big] = \frac{1}{4} \int d^4x\ F_{\mu\nu}^2 + O(a^2), \tag{4}$$

where $U_\Box$ is the product of the gauge fields around a plaquette. The quark action is

$$S_F[U, \bar{q}, q] = a^4 \sum_x \bar{q}(x)(D + m)q(x) = \int d^4x\ \bar{q}(\partial\!\!\!/ + igA\!\!\!/ + m)q + O(a) \tag{5}$$

where the lattice derivative is

$$\begin{aligned} Dq(x) = \frac{1}{2a} \sum_\mu \Big\{ &\gamma_\mu \Big[U_\mu(x)q(x + a\hat{\mu}) - U_\mu^\dagger(x - a\hat{\mu})q(x - a\hat{\mu})\Big] \\ &- \Big[U_\mu(x)q(x + a\hat{\mu}) + U_\mu^\dagger(x - a\hat{\mu})q(x - a\hat{\mu}) - 2q(x)\Big]\Big\}. \end{aligned} \tag{6}$$

This choice gives the unwanted fermionic modes, which are artefacts of the lattice theory[7], masses of order $1/a$, so these should decouple in the continuum limit. It does this by introducing a chiral-symmetry-breaking term of $O(a)$ (from the second term in square brackets in Eq (6)), which is the dominant source of discretisation errors. Since the breaking is proportional to a, chiral symmetry should be restored in the continuum limit. But, the absence of chiral symmetry at non-zero lattice spacing allows additive renormalisation of the quark mass, so that a renormalisation condition must be imposed to define zero quark mass – usually that the pseudoscalar meson mass should vanish at zero quark mass, corresponding to a Goldstone pion. The explicit breaking of chiral symmetry also creates technical problems for the calculation of matrix elements, because operators of different chirality mix.

Note that, although I have explicitly included the lattice spacing, a, simulations are performed in terms of dimensionless variables, in which the quark fields are rescaled, and the quark action is

$$S_F[U,\bar{q},q] = \sum_x \bar{q}(x)\Big\{q(x) - \kappa \sum_\mu \Big[(1-\gamma_\mu)U_\mu(x)q(x+\hat{\mu}) + (1+\gamma_\mu)U_\mu^\dagger(x-\hat{\mu})q(x-\hat{\mu})\Big]\Big\}. \tag{7}$$

The bare parameters are the gauge coupling, $g^2 = 6/\beta$, and the masses of the quark flavours, generically denoted by $m = (1-8\kappa)/2\kappa$. These parameters must be tuned to achieve continuum results corresponding to the physical quark masses.

Staggered Fermions. The alternative staggered-fermion action[8, 9] retains a continuous chiral symmetry and incurs discretisation errors only of $O(a^2)$, just like the gauge action. Unfortunately, it describes degenerate opposite-chirality pairs of quark flavours and so cannot be realistic[5, 7]. Also, it has a complicated flavour structure and large operator renormalisations, which have to be controlled non-perturbatively, making matrix element calculations more difficult than for Wilson quarks.

Hadron Correlators. The spectrum may be computed from hadron correlators of the form

$$\langle \mathcal{O}^\dagger(x)\mathcal{O}(0)\rangle = \frac{1}{Z}\int \mathcal{D}U\,\mathcal{D}\bar{q}\mathcal{D}q\ \mathcal{O}^\dagger(x)\mathcal{O}(0)\ e^{-S_G[U]-S_F[U,\bar{q},q]}, \tag{8}$$

where $\mathcal{O}$ is a gauge-invariant product of quark and gluon fields with the quantum numbers of a specific hadron. For a meson, $\mathcal{O}(x)$ is a bilinear in the quark fields. The simplest possibility is the local product $\bar{q}(x)\Gamma q(x)$. A pseudoscalar meson is generated by using $\Gamma = \gamma_5$ and a vector meson by using $\Gamma = \gamma_i$. However, as the lattice spacing decreases, such local composite fields have decreasing overlap with the meson states, which are of non-zero spatial extent. A bigger overlap with the lightest meson can be achieved using smeared quark fields,

$$\mathcal{O}(t,\vec{x}) = \bar{q}(t,\vec{x})\Gamma \sum_{\vec{y}} \Psi(\vec{x}-\vec{y})q(t,\vec{y}), \tag{9}$$

where Ψ is an approximation to the groundstate wavefunction (which should be gauge covariant, unless the computation is done in a fixed gauge). The nucleon correlator has $\mathcal{O} = \epsilon_{abc}(u^a C\gamma_5 d^b)u^c$, or its smeared version, and the Δ has $\mathcal{O} = \epsilon_{abc}(u^a C\gamma_\mu u^b)u^c$.

The meson correlator is expressed in terms of quark propagators by performing the path integral over the Grassmann variables in Eq (8):

$$\begin{aligned}\langle \bar{q}(x)\Gamma_1 q(x)\bar{q}(0)\Gamma_2 q(0)\rangle = \frac{1}{Z}\int \mathcal{D}U\ \det(D+m)^{N_f}\ e^{-S_G[U]} \\ \times \mathrm{Tr}\ \Gamma_1(D+m)^{-1}_{x0}\Gamma_2(D+m)^{-1}_{0x}.\end{aligned} \tag{10}$$

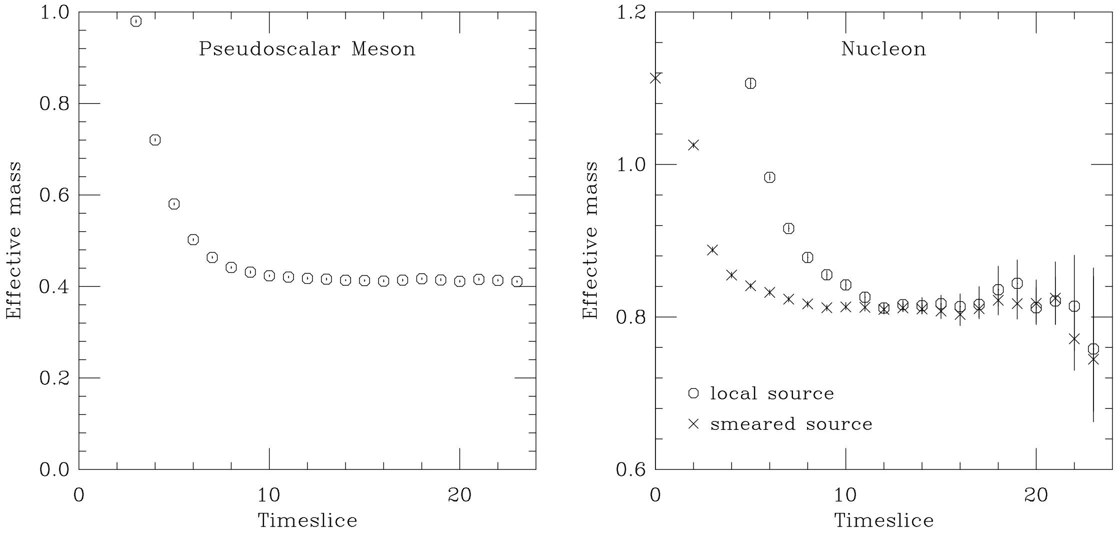

Figure 1. The pseudoscalar meson (left) and nucleon (right) effective masses from a quenched QCD simulation with Wilson quarks at $\beta = 6.0$.

The integration over the gauge fields is performed by Monte Carlo.

The timeslice correlator projects onto zero-momentum eigenstates, $|h_n\rangle$, of the Hamiltonian, $\hat{H}$:

$$\begin{aligned}\sum_{\vec{x}} \langle \mathcal{O}^\dagger(t,\vec{x})\mathcal{O}(0,\vec{0})\rangle &= \sum_{\vec{x}} \langle 0|\hat{\mathcal{O}}(\vec{x})^\dagger e^{-\hat{H}t}\hat{\mathcal{O}}(\vec{0})|0\rangle \\ &= \sum_n \langle 0|\hat{\mathcal{O}}^\dagger|h_n\rangle \frac{e^{-M_n t}}{2M_n}\langle h_n|\hat{\mathcal{O}}|0\rangle \\ &\stackrel{t\to\infty}{\longrightarrow} |\langle 0|\hat{\mathcal{O}}|h_0\rangle|^2 \, \frac{e^{-M_0 t}}{2M_0} \end{aligned} \tag{11}$$

where $|h_0\rangle$ is the lightest hadron state which has a non-zero overlap with $\hat{\mathcal{O}}$, with mass M_0. By fitting the exponential fall-off of the timeslice correlator at large Euclidean times, we can extract the lightest hadron mass, M_0, and the decay-constant matrix element, $\langle 0|\hat{\mathcal{O}}|h_0\rangle$. (Actually, on a periodic lattice, the fit is to a cosh or sinh for mesons and to an exponential for baryons.)

The approach of a timeslice correlator, $C(t)$, to saturation by the lightest hadronic state can be displayed by plotting the effective mass,

$$M_{\rm eff}(t) = \log \frac{C(t)}{C(t+1)} \tag{12}$$

versus timeslice, t, examples of which are shown in Fig 1. On a finite lattice, a systematic error is introduced in the hadron mass estimates, because of the contamination of the timeslice correlator, Eq (11), by excited states. This can be reduced by choosing the smearing function, Ψ, to maximise the overlap with the state of interest, as can be seen for the nucleon in Fig 1, and by using multi-exponential fits to absorb some of the excited state contributions. Unfortunately, the statistical error grows at large times for any hadron other than the pion, typically,

$$\frac{\text{noise}}{\text{signal}} \sim e^{(M_{\rm meson}-M_\pi)t}, \quad \text{or} \quad \sim e^{(M_{\rm baryon}-3M_\pi/2)t} \tag{13}$$

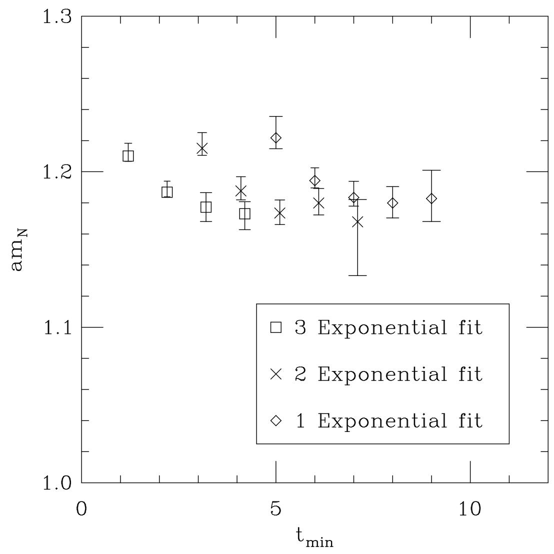

Figure 2. Nucleon mass from 1-, 2- and 3-exponential fits to the timeslice correlator as the minimum time, $t_{\rm min}$, in the range of timeslices included in the fit, is increased[10].

and so the range of timeslices available is limited. The number of exponentials and the range of timeslices are chosen to minimise the contamination, while maintaining a good signal, which can be judged to occur when the result of the fit becomes independent of the minimum timeslice included, as shown in Fig 2.

Continuum Limit. The hadron masses extracted from the fitted data are dimensionless functions of g (at fixed quark mass, which I take to be $m = 0$ for simplicity). The lattice spacing in physical units is then,

$$a(g) = \frac{M_h(g)}{M_h^{\rm expt}} \tag{14}$$

and $a = 0$ corresponds to the critical point $M_h(g^*) = 0$, for all hadrons, h.

It is not necessary to reach $a = 0$ directly. Instead, a needs only to be small enough that the masses scale:

$$\frac{M_h(g)}{M_{h'}(g)} = \text{constant} = \frac{M_h^{\rm expt}}{M_{h'}^{\rm expt}}. \tag{15}$$

This implies a universal dependence on the gauge coupling,

$$M_h(g) = c_h\ f(g) \tag{16}$$

and the existence of a cut-off independent mass,

$$\Lambda_{\rm QCD} = \frac{1}{a} f(g). \tag{17}$$

Then, from Eq (14), the requirement that

$$\frac{d}{da} M^{\rm expt} = 0 \tag{18}$$

implies that

$$f(g) = \exp - \int^g \frac{dg'}{\beta(g')}, \qquad \beta(g) = -a\frac{dg}{da}. \tag{19}$$

Asymptotic freedom tells us that $a = 0$ at $g = 0$. So $\beta(g)$ may be reliably computed in perturbation theory, with the result that

$$\beta(g) = -\beta_0 g^3 - \beta_1 g^5 - \ldots, \qquad \beta_0 = \frac{33 - 2N_f}{3(16\pi^2)}. \tag{20}$$

Combining Eqs (17), (19) and (20), we know the behaviour of masses as g is tuned towards zero. In practice, mass ratios from the current best data still have a lattice-spacing dependence and are not yet scaling, i.e.,

$$\frac{M_h(g)}{M_{h'}(g)} = \text{constant} + O(a^p). \tag{21}$$

But we are close enough for the a^p dependence to be extrapolated away, with sufficient confidence, using the theoretically-expected exponent, p.

The Monte Carlo Method for Quenched QCD

The Algorithm. The idea is to approximate the path integral over the gauge fields in Eq (10) by an average over a finite ensemble of gauge configurations, $\{U^{(n)}|n = 1, \ldots, N_{\text{config}}\}$, drawn from the probability distribution

$$\mathcal{P}[U] = \frac{1}{Z} \det(D[U] + m)^{N_f} e^{-S_G[U]}. \tag{22}$$

Unfortunately, the inclusion of the determinant greatly increases the computational cost, typically by a factor of a thousand at current parameter values, and so it is usually ignored in what is called the quenched approximation.

An expectation value, such as the meson correlator, is approximated by

$$\langle \bar{q}(x)\Gamma_1 q(x)\bar{q}(0)\Gamma_2 q(0)\rangle \simeq \frac{1}{N_{\text{config}}} \sum_{n=1}^{N_{\text{config}}} \text{Tr}\ \Gamma_1 (D[U^{(n)}] + m)^{-1}_{x0} \Gamma_2 (D[U^{(n)}] + m)^{-1}_{0x}. \tag{23}$$

Provided the gauge configurations are statistically independent, the error in the mean decreases like $1/\sqrt{N_{\text{config}}}$. There is some subtlety here: because the ensemble is generated in a Markov process, which converges to the distribution in Eq (22) after some number of steps (which must be discarded), successive configurations are correlated. So the ensemble must be built up from sufficiently widely separated configurations. These days, the statistical errors are largely under control and a sophisticated statistical analysis is employed to account for correlations between different quantities computed using the same ensemble of configurations.

Quark Propagators. The quark propagator,

$$G_{x0}[U^{(n)}] = (D[U^{(n)}] + m)^{-1}_{x0} \tag{24}$$

for a given gauge configuration, $U^{(n)}$, is obtained by solving the large sparse system of linear equations,

$$(D[U^{(n)}] + m)_{xy} G_{y0} = \delta_{x0}. \tag{25}$$

Because of the high computational cost, considerable effort has gone into finding efficient algorithms for this[11]. These are iterative in nature and, at fixed quark mass, the cost scales with the number of lattice sites.

Quenched Approximation. Replacing $\det(D+m)$ by a constant, its mean value, becomes valid in the limit of large quark mass. In Feynman-diagram language, it corresponds to omitting virtual quark loops. There are two ways of viewing Quenched QCD (QQCD):

- as an effective theory for QCD, in which its bare parameters at fixed lattice spacing are chosen empirically to best match experiment (and by assumption QCD);
- as a peculiar type of quantum field theory in its own right, which almost certainly is pathological in the limit $m \to 0$.

When doing phenomenology the first approach is taken. Some dynamical quark effects are incorporated in the choice of parameters. This is why QQCD has provided such a successful basis for QCD phenomenology, and why it has taken so long to reach the point where quenching errors dominate for most physical quantities. The second approach can provide insight as to when to expect this effective theory to fail.

Mass Ratios and the Edinburgh Plot

QCD should have a well-defined continuum limit for any specific choice of the quark masses. Simulations are usually carried out for a range of quark masses and the data extrapolated/interpolated to the physical quark mass values. For simplicity, if we consider a single quark flavour, then we can fix the quark mass by fixing M_{PS}/M_V, say. Then continuum physics corresponds to all other mass ratios being independent of g for g small enough.

The spectra obtained at different lattice spacings may be compared using the Edinburgh Plot[12] in which one mass ratio, usually M_N/M_V is plotted versus the ratio used to fix the quark mass, usually M_{PS}/M_V. Scaling corresponds to these data falling on a universal curve. Typically, the data are compared with a phenomenological quark model[13],

$$M_{\text{baryon}} = M_b + \sum_{i=1}^{3} m_i + \xi_b \sum_{i>j} \frac{\vec{s}_i \cdot \vec{s}_j}{m_i m_j} \tag{26}$$

$$M_{\text{meson}} = M_m + \sum_{i=\bar{q},q} m_i + \xi_m \frac{\vec{s}_{\bar{q}} \cdot \vec{s}_q}{m_{\bar{q}} m_q} \tag{27}$$

where the parameters, M, m and ξ are taken from experiment. This is expected to be a good model for large quark mass, but does not have the correct chiral behaviour.

The original Edinburgh Plot[12] is shown in Fig 3. Evidently, as was concluded at the time, the data does not scale down to $\beta = 5.7$. The corresponding plot today, also shown in Fig 3, includes the same lattice spacings, but an improved lattice formulation with reduced discretisation error, lattices twice the linear size and much higher statistics. The error bars are much smaller and now the data scale at fixed quark mass. Notice that this progress has been achieved without significantly reducing the lattice spacing.

THE CHOICE OF PARAMETERS

The Computational Scaffolding

Finite volume. Numerical simulations are done in a finite volume, so that the number of degrees of freedom is finite and they can be stored in the finite memory of a

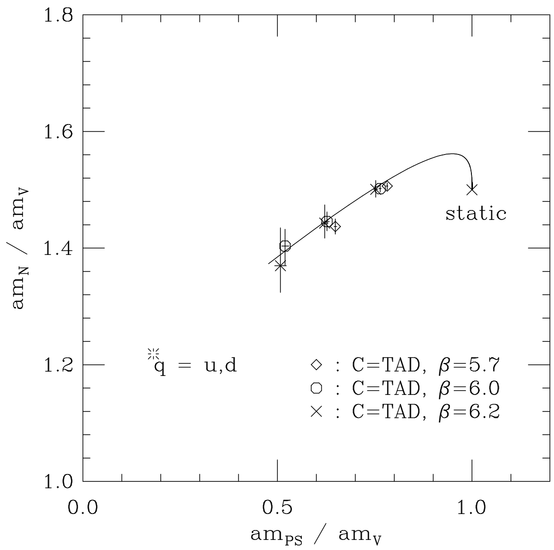

Figure 3. The original 1985 Edinburgh plot[12] (left), showing data from quenched simulations on 8^3, 10^3 and 16^3 spatial lattices, at two lattice spacings, and the 1997 Edinburgh plot (right) showing scaling at fixed m_{PS}/m_V using the tadpole-improved action.

computer! Ideally, with enough computer power, we could obtain all physical quantities in a range of physical volumes and extrapolate the results to the infinite-volume limit. Unfortunately, we are far from this situation, and do not really understand the dependence on lattice size for the existing range of data. Finite-size effects are expected to fall exponentially with lattice size[14], so it is reasonable, and the best we can hope for at present, to increase the lattice size until they are obscured by the statistical errors. For QQCD, a linear dimension of around 2.5 fm seems to be large enough[15] for the nucleon. In full QCD, finite-size effects are expected to be larger, so larger volumes will probably be needed, but existing data is too sparse to conclude anything.

Non-zero lattice spacing. Considerable progress has been made recently in systematically exploring the discretisation errors due to non-zero lattice spacing in QQCD. Today's simulations span a range of lattice spacings corresponding to momentum cutoffs extending from $a^{-1} \simeq 1.1$ GeV at $\beta = 5.7$ to 3.5 GeV at $\beta = 6.4$. These numbers are only a rough guide, of course, because estimates from Eq (14) using different hadrons, do not have to agree in the quenched theory. There is evidence from matrix-element calculations that discretisation errors, due to the chiral-symmetry-breaking term in the Wilson action may be large in this range, eg as much as 30% in the normalisation of the vector current, and over 50% when the PCAC relation,

$$\partial_\mu A^a_\mu = 2mP^a \tag{28}$$

is sandwiched between different external states[16]. So reducing these errors has been the major goal in recent years. Significantly reducing the lattice spacing itself is not a practical option!

Computational cost. In QQCD, for an N^4 lattice, the computational cost grows like N^6 at fixed physical length scales ($aM_\pi N$ = constant) and fixed statistical error (it comprises two factors, the lattice volume and $1/(aM_\pi)^2$, where the latter comes from either the random walk by which the Monte Carlo algorithm explores the physical length scale, or the condition number of the fermion matrix). So, to reduce the lattice spacing by a factor 2 costs around 64 times more computer power. This is a compelling argument for trying to improve the lattice formulation by introducing irrelevant terms which cancel the leading discretisation errors, even though these terms have coefficients which have to be determined non-perturbatively. For dynamical quarks the computational cost grows like $N^{10.5}$, and improvement is the only hope, short of an algorithmic miracle!

Improvement and Irrelevant Parameters

Local effective theory. The effects of the leading discretisation errors in Eqs (4) and (5) on on-shell quantities (particle energies, matrix elements of local composite operators, etc) can be systematically eliminated by means of the Symanzik improvement programme[17], in which higher-dimension operators are added to the lattice action and to the composite fields in correlation functions[18].

Close to the continuum limit, the lattice action, Eq (3), may be expanded around the continuum action, $S_{\rm ctm}$,

$$S = S_{\rm ctm} + a\int d^4x\ \mathcal{L}_1(x) + O(a^2) \tag{29}$$

where $\mathcal{L}_1$ is a linear combination of dimension 5 composite fields:

$$\mathcal{O}_1 = \bar q\sigma_{\mu\nu}F_{\mu\nu}q, \tag{30}$$
$$\mathcal{O}_2 = \bar q D_\mu D_\nu q + \bar q\ \overleftarrow{D}_\mu \overleftarrow{D}_\nu\ q \tag{31}$$
$$\mathcal{O}_3 = m\mathrm{Tr}\ F_{\mu\nu}F_{\mu\nu} \tag{32}$$
$$\mathcal{O}_4 = m\{\bar q\gamma_\mu D_\mu q - \bar q\ \overleftarrow{D}_\mu\ \gamma_\mu q\} \tag{33}$$
$$\mathcal{O}_5 = m^2\bar q q. \tag{34}$$

Similarly, any renormalised composite field, $Z_\phi\phi(x)$, built from the quark and gluon fields, can be expanded in terms of local composite fields,

$$Z_\phi\phi(x) = \phi_0(x) + a\phi_1(x) + O(a^2). \tag{35}$$

The classical field equations can be used to find linear combinations of the fields in Eqs (30)–(34) which vanish, and a linearly-independent basis is $\mathcal{O}_1$, $\mathcal{O}_3$ and $\mathcal{O}_5$.

Improved lattice action. A lattice action in which $\mathcal{L}_1$ vanishes can be obtained by adding a counterterm of the form

$$a^5\sum_x\Big\{c_1\hat{\mathcal{O}}_1(x) + c_3\hat{\mathcal{O}}_3(x) + c_5\hat{\mathcal{O}}_5(x)\Big\} \tag{36}$$

where $\hat{\mathcal{O}}_k$ is some lattice representation of $\mathcal{O}_k$[19]. The $O(a)$ counterterms in $\hat{\mathcal{O}}_3$ and $\hat{\mathcal{O}}_5$ renormalise the bare coupling and mass. Hence, the $O(a)$-improved action involves one additional term, the so-called 'clover term',

$$S_{\rm SW} = S[U,\bar q,q] + a^5\sum_x \bar q(x)\frac{ic\kappa}{2}\sigma_{\mu\nu}F_{\mu\nu}(x)q(x) \tag{37}$$

where the name derives from the four plaquettes used to approximate $F_{\mu\nu}$, which was first written down by Sheikholeslami and Wohlert[20, 21].

Improved axial current. Composite fields such as the isovector axial current and the pseudoscalar density,

$$A^a_\mu(x) = \bar{q}(x)\gamma_\mu\gamma_5\frac{\tau^a}{2}q(x) \tag{38}$$

$$P^a(x) = \bar{q}(x)\gamma_5\frac{\tau^a}{2}q(x), \tag{39}$$

where τ^a is a Pauli matrix acting on flavour, must also be improved if all $O(a)$ effects are to be removed from their matrix elements. Again, the classical field equations may be used to eliminate some of the field combinations, and we find that for the axial current only one additional term is needed[19]:

$$A^{a,\text{imp}}_\mu(x) = A^a_\mu(x) + \frac{c_A}{2}\Big[P^a(x+a\hat{\mu}) - P^a(x-a\hat{\mu})\Big]. \tag{40}$$

A^a_μ must be renormalised if it is to obey the correct current algebra[22]. If a mass-independent renormalisation scheme is used to compute the matching factor $Z_A(g^2)$, then the renormalised improved axial current receives an additional term of $O(ma)$[18]:

$$A^{a,\text{ren}}_\mu(x) = Z_A(g^2)\Big(1 + b_A(g^2)am\Big)A^{a,\text{imp}}_\mu(x). \tag{41}$$

The coefficients c, c_A, b_A, etc, are functions of g^2 and are determined by imposing improvement conditions.

Choice of improvement coefficients. At tree-level in perturbation theory,

$$c = 1 \tag{42}$$

$$c_A = 0 \qquad \text{(tree level)} \tag{43}$$

$$b_A = 1 \tag{44}$$

and it can be shown that the leading discretisation errors are reduced to $O(g^2a)$, provided the quark fields are 'rotated' by an amount of $O(am)$, corresponding to the b_A term in Eq (41)[21].

Perturbative expansions in terms of the bare coupling are useless for most quantities, because of large contributions from tadpole graphs. If these tadpole contributions are treated non-perturbatively, eg by writing $U_\mu = u_0[1 + igaA_\mu + \ldots]$ with $u_0 = \langle\frac{1}{3}(\text{Tr}\, U_\Box\rangle^{1/4}$ from the simulations, and the perturbative expressions are adjusted to remove the one-loop contribution from u_0, then the perturbative estimates are much more reliable[23]. The mean-field, or tadpole, prescription for the action is to replace

$$U_\mu(x) \to \frac{U_\mu(x)}{u_0} \tag{45}$$

everywhere, and then to use perturbation theory (excluding the perturbative contribution from u_0) for the coefficients, ie,

$$g^2 = \tilde{g}^2 u_0^4, \qquad \kappa = \frac{\tilde{\kappa}}{u_0}, \qquad c = \frac{\tilde{c}}{u_0^3} \tag{46}$$

where $\tilde{\kappa}_c$ and $\tilde{c}$ should be close to their perturbative values of $1/8$ and 1, respectively. In other words,

$$c = \frac{\tilde{c}}{u_0^3}, \qquad \tilde{c} = 1 \tag{47}$$

$$c_A = 0 \qquad\qquad \text{(tadpole)} \tag{48}$$

$$b_A = \frac{\tilde{b}_A}{u_0}, \qquad \tilde{b}_A = 1 \tag{49}$$

and the tadpole-improved axial vector current is[24, 25, 26],

$$A_\mu^{a,\mathrm{ren}}(x) = Z_A\, 2\kappa u_0 \Big(1+\frac{am}{u_0}\Big) A_\mu^a(x) \quad \text{(tadpole)} \tag{50}$$

$$Z_A = 1 + \Big(\frac{1}{12} - 0.116458\Big)\frac{g^2}{u_0^4}. \tag{51}$$

The Alpha Collaboration have determined c and c_A non-perturbatively[27] by requiring that the PCAC relation, Eq (28), holds irrespective of the states between which it is sandwiched[19]. The resulting best fit to the numerical data is

$$c = \frac{1 - 0.656g^2 - 0.152g^4 - 0.054g^6}{1-0.922g^2} \quad \text{(non-perturbative, } g^2 \le 1) \tag{52}$$

$$c_A = -0.00756g^2\,\frac{1-0.748g^2}{1-0.977g^2} \tag{53}$$

$$b_A = 1 + 0.1522\, g^2 \quad \text{(1-loop perturbation theory[28])} \tag{54}$$

The non-perturbative values should remove all $O(a)$ discretisation errors, whereas this is not guaranteed using the tadpole prescription. In both cases, the hope is that the remaining a dependence is weak enough to be extrapolated away with confidence.

Relevant Parameters

QCD has N_f+1 free parameters, the quark masses and the gauge coupling. So N_f+1 dimensionful quantities, usually hadron masses, must be taken from experiment. One of these determines the lattice spacing in physical units, or, equivalently, the QCD scale, Λ_{QCD}, via the usual dimensional transmutation. The others determine the renormalised quark masses.

Chiral behaviour. Present day simulations are carried out for quark masses in the vicinity of m_s or higher. There are three reasons for this:

- The linear equation solvers for computing quark propagators typically have a condition number $\propto 1/(aM_{PS})^2 \propto 1/am$, so that the number of iterations grows linearly as the quark mass decreases and the computations become too expensive.
- Finite-size effects are likely to be large when the pseudoscalar meson mass is small and these would have to be modelled.
- Quenched QCD is pathological in the limit $m \to 0$, so the simulations cannot be regarded as a good approximation to QCD.

Consequently, the results for physical quantities have to be extrapolated in m from $m \simeq m_s$, where they are computed, to $m = m_{u,d}$.

The form of this extrapolation is given by leading-order chiral perturbation theory[29]. This assumes that the shift in mass away from the $m=0$ limit is given by the matrix element of the quark mass term in the action:

$$\delta M = \frac{\langle|m\bar{q}q|\rangle}{\langle|\rangle} = \frac{m}{2M}\langle\bar{q}q\rangle, \tag{55}$$

using the covariant normalisation of states, ie,

$$\delta M^2 = m\langle\bar{q}q\rangle. \tag{56}$$

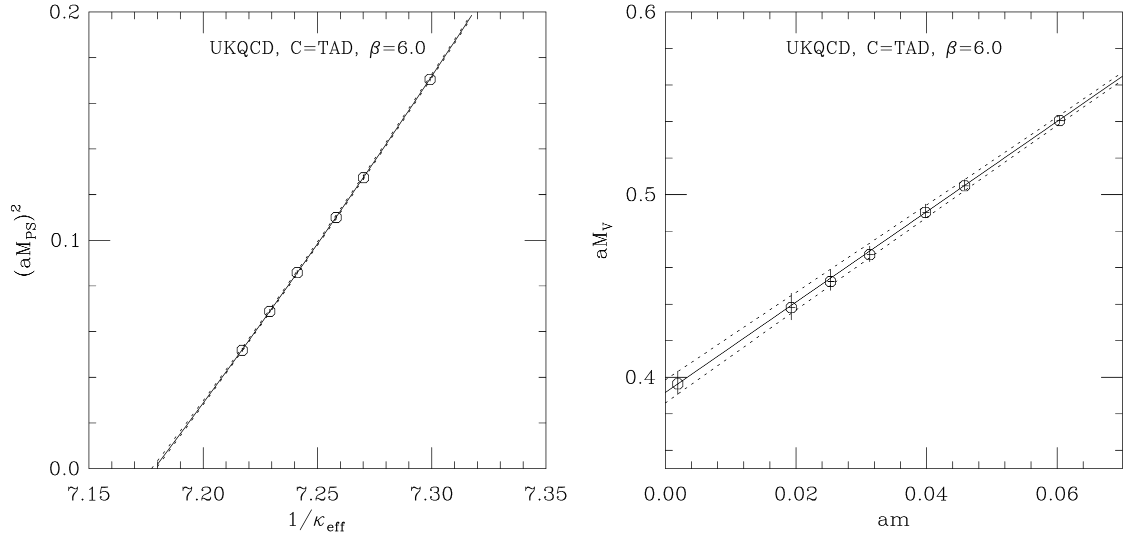

Figure 4. The squared pseudoscalar meson mass in lattice units versus the sum of the quark masses, $1/\kappa_{\rm eff} = 1/2\kappa_1 + 1/2\kappa_2$, (left) and the vector meson mass versus quark mass, am, (right) from a quenched simulation with tadpole-improved Wilson quarks at $\beta = 6.0$.

Assuming the pseudoscalar meson's mass comes solely from this mechanism,

$$(aM_{PS})^2 = C_{PS}\, am \tag{57}$$

whereas, for hadrons whose masses do not vanish at $m = 0$,

$$aM_h = A_h + B_h\, am. \tag{58}$$

For hadrons made of non-degenerate quarks, m is the average quark mass. Chiral perturbation theory is believed to be reliable for quark masses up to that of the strange quark. Eq (57) and (58) should be used also for QQCD if we are using it as an effective theory.

The numerical simulation data for Wilson quarks is consistent with this picture, although chiral symmetry is broken explicitly at non-zero lattice spacing. As a consequence, there is no symmetry to prevent additive renormalisation of the quark mass. We find that the square of the pseudoscalar meson mass vanishes at $m = m_c$ (equivalently, $\kappa = \kappa_c$), as shown in Fig 4. For this set of data, slight curvature is observed over this range of quark masses, which extends to just above the strange quark mass, and the best fit is to,

$$(aM_{PS})^2 = C_{PS}\, am + D_{PS}(am)^2 \tag{59}$$

where

$$am = \frac{1}{2\kappa_{\rm eff}} - \frac{1}{2\kappa_c}. \tag{60}$$

Also shown in Fig 4 is the fit of Eq (58) to data for the vector meson mass. The vanishing of the pseudoscalar meson mass at non-zero lattice spacing indicates a critical point of the Wilson theory[30]. The associated critical exponents determine the rate at which the pseudoscalar meson mass vanishes with quark mass, and the square-root behaviour of Eq (57) corresponds to mean-field exponents.

The values chosen for the quark masses in Fig 4 are too large to expose quenching effects, but it is interesting to compute the modification to the chiral behaviour due to QQCD.

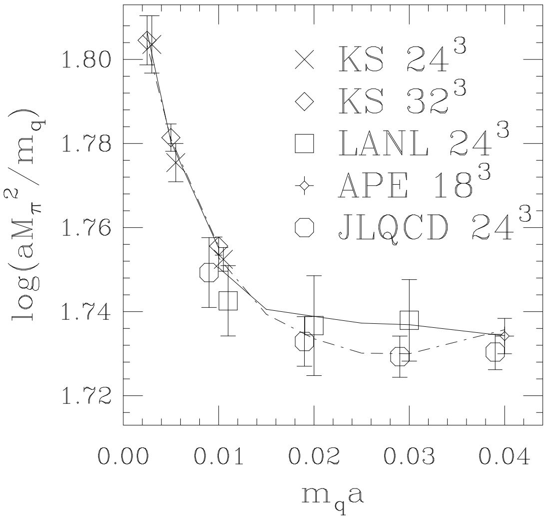

Figure 5. The observed chiral behaviour of the pseudoscalar meson mass in QQCD[32].

Quenched chiral perturbation theory. There are two distinct quenching effects[31].

1. Quenching removes loops which, at the underlying quark level, involve internal quark loops. This changes the values of the coefficients in the chiral expansion and may remove some terms completely.

2. Because of the absence of an anomaly, the η' remains light in QQCD, so there are new contributions coming from η' loops. Some of these are singular in the chiral limit. If these terms are large, then one can be sure that quenching errors are large. Consequently, it is necessary to carry out simulations at large enough quark masses for these terms to be negligible.

The η' loops modify the behaviour of the pseudoscalar meson mass in the chiral limit,

$$M_{PS}^2 = C'_{PS} m \Big[1 + \delta \ln\Big(\frac{\Lambda^2}{M_{PS}^2}\Big)\Big] \tag{61}$$

where $\delta \simeq 0.2$, so that

$$\frac{M_{PS}^2}{m} \propto m^{-\frac{\delta}{1+\delta}} \tag{62}$$

and this divergence has been observed in simulations, as shown in Fig 5[32].

Renormalised quark masses. The light quark masses are amongst the most poorly known parameters of the Standard Model. The Particle Data Book[33] gives $2 \le m_u \le 8$, $5 \le m_d \le 15$, and $100 \le m_s \le 300$ MeV (evaluated in the $\overline{\rm MS}$ scheme at $\mu = 1$ GeV). Chiral perturbation theory[29, 34] relates their masses to those of the pseudoscalar mesons, but only predicts dimensionless ratios, eg, $2m_s/(m_u + m_d) = 25$ at lowest order, and 31 at next order.

Lattice QCD can provide a precise determination, because it directly relates input quark masses to output hadron masses. However, since electromagnetic effects are not included in the simulations, we can only calculate the isospin symmetric mass

$\bar{m} = (m_u + m_d)/2$. The lattice scale is usually taken from $M_\rho = 770$ MeV, then $\bar{m}$ is fixed by the isospin-averaged value $M_\pi = 137$ MeV, and m_s is fixed by one of $M_K = 495$ MeV, $M_{K^*} = 894$ MeV and $M_\phi = 1020$ MeV.

The $\overline{\mathrm{MS}}$ mass at scale μ is related to the lattice mass by[35]

$$\begin{aligned} m_{\overline{\mathrm{MS}}}(\mu) &= Z_m(\mu a) m(a) \\ &= \Big\{1 - \alpha_s\Big[\gamma_0 \ln(\mu a) - C_m\Big]\Big\} m(a) \\ &= \Big\{1 - \tilde{\alpha}_s\Big[\gamma_0 \ln(\mu a) - \tilde{C}_m\Big]\Big\} \frac{m(a)}{u_0}. \end{aligned} \tag{63}$$

Here $Z_m = Z_S^{-1}$ is the mass renormalisation, at one-loop order, relating the lattice and continuum regularisation schemes. It is computed by demanding that on-shell Green functions calculated with both regulators be equal[36, 37]. $\gamma_0 = 2/\pi$ is the leading quark mass anomalous dimension. In the last part of Eq (63), the tadpole-improved mass is used, Eq (46), and the perturbative matching adjusted to remove the one-loop contribution to u_0. The lattice mass in Eq (63) is taken to be

$$m(a) = \frac{1}{a}\Big(\frac{1}{2\kappa} - \frac{1}{2\kappa_c}\Big) \tag{64}$$

for Wilson quarks, and is the bare mass in the lattice action for staggered quarks. There is some freedom in the precise choice of scale, $1/a \le \mu \le \pi/a$, in Eq (63) at which to match the continuum and lattice theories, and in the corresponding value of α_s (or $\tilde{\alpha}_s$). The usual choice follows the approach of Lepage and Mackenzie, with $\mu = q^*$, the dominant momentum scale in the loop integration, and $\tilde{\alpha}_s = \alpha_{\overline{\mathrm{MS}}}(q^*)$[23]. Once $m_{\overline{\mathrm{MS}}}(\mu)$ has been computed, its value at any other scale Q is given by the two-loop running[38].

It turns out that the resulting quark masses are not very sensitive to tadpole effects (because the operators involved only contain one link variable), or to the choice of q^*. For Wilson quarks the one-loop contribution to Z_m is small, so the perturbative estimate of the renormalisation factor is likely to be reliable. But for staggered quarks the one-loop term is large, regardless of whether tadpole improvement is used, and the renormalisation factor is the major source of uncertainty. However, extrapolation of the lattice data to the continuum limit should remove any systematic error in the renormalisation prescription.

The u and d quark masses are determined by solving Eq (57) and Eq (58) with $m_h = m_V$, for $m = \bar{m}$, given $M_{PS} = M_\pi$ and $M_V = M_\rho$. The data from a range of simulations are shown in Fig 6. The expected leading term in the discretisation error is $O(a)$ for Wilson, $O(g^2 a)$ for tree-level improved (clover), and $O(a^2)$ for staggered quarks. This leading behaviour is used to extrapolate to $a = 0$, giving a consistent continuum limit of[35]

$$\bar{m}_{\overline{\mathrm{MS}}}(2\text{ GeV}) = 3.4 \pm 0.4 \pm 0.3\text{ MeV}, \tag{65}$$

where the first error is the largest of the extrapolation errors and the second is due to the uncertainty in the scale. The data for the s quark mass in QQCD, obtained by fixing $M_V(m_s) = M_\phi$, are also shown in Fig 6. The Wilson data again show large $O(a)$ effects, although a consistent extrapolation to $a = 0$ is possible for both the Wilson and staggered data, giving[35]

$$m_{s,\overline{\mathrm{MS}}}(2\text{ GeV}, M_\phi) = 100 \pm 21 \pm 10\text{ MeV}. \tag{66}$$

This is at the lower end of the expected range of values, but the ratio $m_s/\bar{m}$ is in good agreement with second-order chiral perturbation theory.

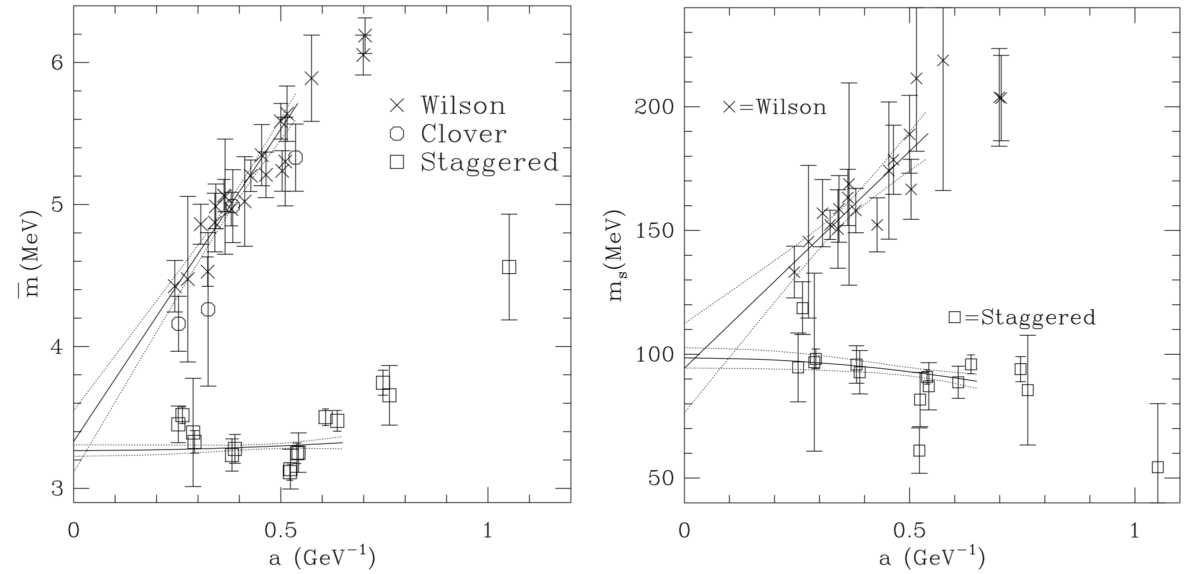

Figure 6. The behaviour with lattice spacing of $\bar{m}_{\overline{\mathrm{MS}}}(2\ \mathrm{GeV})$ obtained from M_π (left) and $m_{s,\overline{\mathrm{MS}}}(2\ \mathrm{GeV})$ obtained from M_ϕ (right) in QQCD with the scale set by M_ρ[35].

LIGHT HADRONS IN QUENCHED QCD

Early Results with Improved Actions

As an example of the present state of the art, I now present UKQCD's latest results for the spectrum of light hadrons and pseudoscalar decay constants in QQCD[3], obtained from simulations at $\beta = 5.7$, 6.0 and 6.2, which enable us to compare extrapolations to zero lattice spacing using the tadpole and the non-perturbative prescriptions for the clover coefficient. We find good agreement between the continuum estimates, which suggests that the extrapolation is under control. Although our data is at a fixed, and unfortunately rather small, box size with linear dimension of only about 1.7 fm, we also have data for a larger volume on the coarsest lattice for each improvement prescription and this gives us a check of finite-size effects.

At both volumes, our ensembles at $\beta = 6.0$ for the non-perturbatively-improved action contain a small number of exceptional configurations, in which the fermion matrix has a (near) zero eigenvalue[39]. For these configurations, which have been excluded from our analysis, the quark propagators at our lightest κ value fail to converge using several different solvers, although we have successfully converged some of them with a QMR algorithm[11]. The resulting pseudoscalar-meson timeslice correlator does not have a simple exponential decay from $t = 0$, as in Eq (11), and would distort the Monte Carlo average. Such zero modes are an artefact of the quenched approximation, because they appear with zero probability in the ensemble for full QCD (the determinant in Eq (22) would vanish), and so it is legitimate to omit them from the QQCD ensemble.

The Edinburgh plot for the light-hadron spectrum at our chosen quark mass values and using tadpole improvement is shown in Fig 3. The results using non-perturbative improvement are similar. In both cases, the mass ratios scale at fixed quark mass, defined by the value of M_{PS}/M_V. As shown in Fig 4, we observe slight curvature in our data for M_{PS}^2 versus quark mass and so we extrapolate to the chiral limit using Eq (59). For all other masses, our data are consistent with linear behaviour and we use Eq (58).

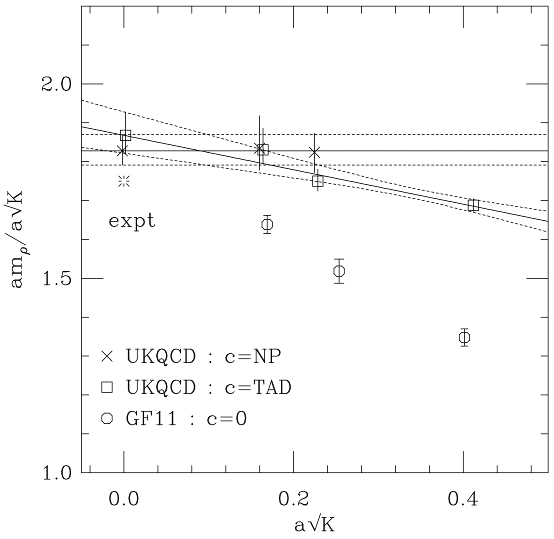

Figure 7. M_ρ versus lattice spacing, with the scale set by the string tension (points have been slightly displaced horizontally for clarity).

The tadpole-improvement prescription[23] is expected to reduce the leading discretisation error in physical quantities, but not to eliminate it completely, so some $O(a)$ dependence should remain in this data. In contrast, the leading lattice-spacing dependence for the non-perturbative improvement prescription[18] should be $O(a^2)$. In comparing the continuum extrapolations for our two data sets, we should work to a consistent order in a, ie, either we ignore $O(a^2)$ corrections in both sets of data, or we include them in both. Unfortunately, we only have three different lattice spacings for the tadpole-improved data and two for the non-perturbatively improved data, so only the first option is available to us. Hence, in the following, I will compare the results from linearly extrapolating the tadpole-improved data to $a = 0$, with the results from fitting the non-perturbatively improved data to a constant. This latter choice certainly underestimates the error in the continuum limit, but I shall be concerned only with showing consistency between the two continuum estimates, and this turns out to be remarkably good even within the unrealistically small errors. I note that, as a consequence of this agreement, we could fit all five data consistently to $O(a^2)$, with a single continuum value, to obtain a more reliable error estimate for the continuum limit.

Meson Masses

The lattice-spacing dependence of the ρ mass in units of the square root of the string tension, is shown in Fig 7. As expected, the tadpole-improved data are consistent with linear behaviour, whereas the dependence of the non-perturbatively improved data is weaker and consistent with a constant. The continuum extrapolations agree. This limit agrees with a linear extrapolation of GF11's data for the Wilson fermion action[2], which show a much stronger lattice-spacing dependence.

The strange quark mass can be fixed using any one of M_K, M_{K^*} and M_ϕ. These prescriptions are inconsistent in quenched QCD at fixed lattice spacing[24, 35]. In other words, the strange meson spectrum, at non-zero lattice spacing, is inconsistent with experiment. However, we find consistent results in the continuum limit. For example,

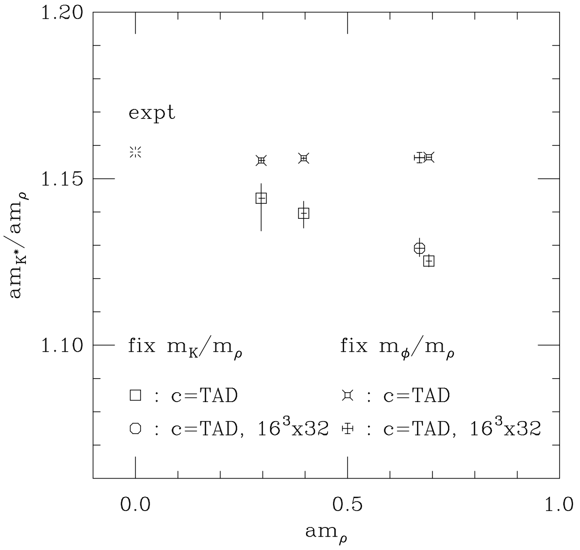

Figure 8. K^* mass in units of M_ρ, obtained from two different definitions of the strange quark mass.

Fig 8 shows our tadpole-improved estimates for the K^* mass, obtained using the K and the ϕ to define m_s. Although there are big differences between the results at non-zero lattice spacing, the continuum extrapolations are consistent with each other and with experiment. Fig 8 also shows results in a bigger volume at the coarsest lattice spacing, which indicate that finite-size effects for mesons are small.

Quark Masses

The light-quark masses at 2 GeV obtained with tadpole improvement are shown in Fig 9. Our results using the non-perturbative value of c are essentially identical to these, because the c values are almost the same and we do not yet have a non-

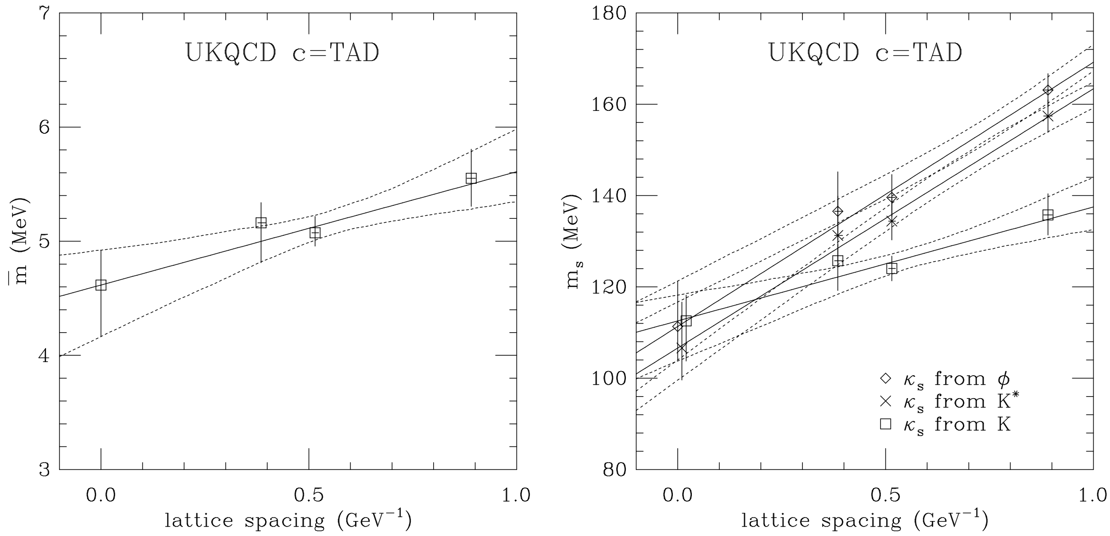

Figure 9. Continuum extrapolations of the light-quark $\overline{\rm MS}$ masses at 2 GeV, using tadpole improvement.

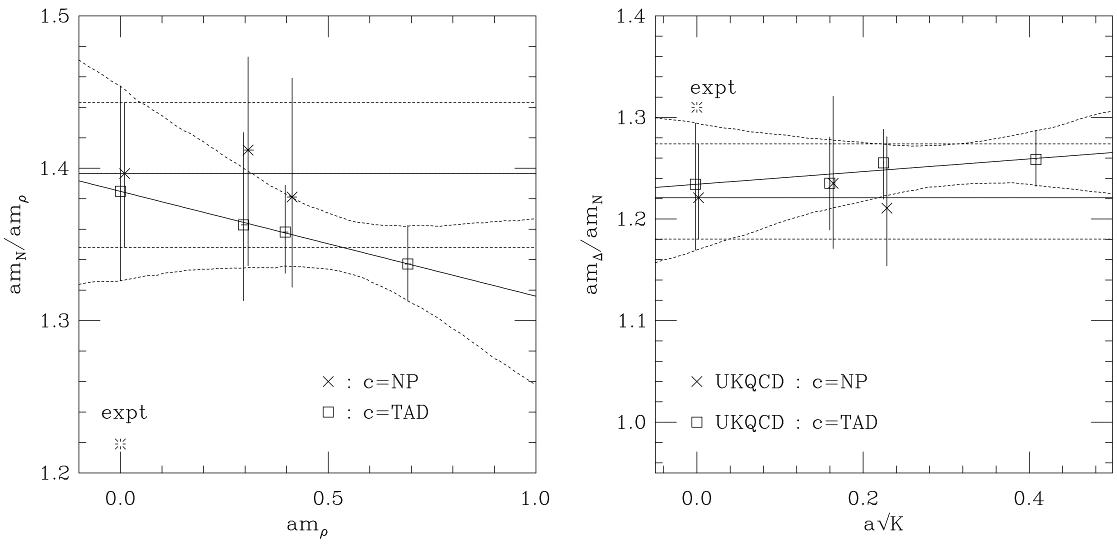

Figure 10. Continuum extrapolations of the nucleon mass in units of M_ρ (left) and the ratio of the Δ mass to the nucleon mass (right).

perturbative determination of Z_m, so we have to use the tadpole-improved values. Our u and d masses are 2σ above the estimate, Eq (65), based on world data, but this is not significant given the spread of data in Fig 6. Our result for m_s does agree with world data (Eq (66)), and confirms our observation from the strange meson spectrum that differences in the definitions of m_s at fixed lattice spacing, go away in the continuum limit.

Baryon Masses

Continuing this analysis for the baryons gives a similar picture of consistent continuum extrapolations for the two improvement schemes. This can be seen for the nucleon mass in Fig 10, although the continuum value appears to disagree with experiment (a bigger discrepancy is obtained if we use the scale from the string tension, rather than from M_ρ).

The ratio of the Δ mass to the nucleon mass, also shown in Fig 10, is only weakly dependent on lattice spacing (in both improvement schemes) and the continuum estimate is, in this case, in good agreement with experiment.

It is necessary to confirm that the baryons are not affected by the small volume of the lattice. Our results on a lattice of twice the linear size show that there is no discernable effect, given the size of our statistical errors.

Pseudoscalar Meson Decay Constants

The pseudoscalar meson decay constant, f_{PS}, is defined by the matrix element of the axial vector current,

$$\langle 0|A_0^{\rm ren}|PS\rangle = if_{PS}M_{PS}, \tag{67}$$

which is computed from the ratio of the axial-pseudoscalar and the pseudoscalar-pseudoscalar correlation functions, cf Eq (11). The tadpole-improved axial vector current is given in Eq (50). In the non-perturbatively improved scheme, the lattice axial vector and pseudoscalar currents are mixed (Eq (40)). This effect appears to be significant at our lattice spacings, but unfortunately, at the time of writing, the

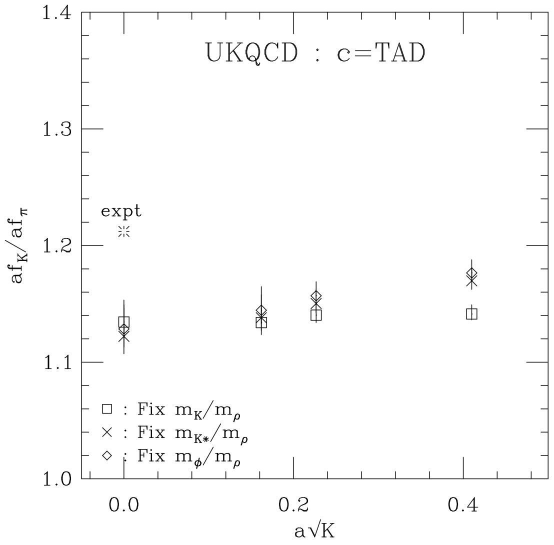

Figure 11. Lattice-spacing dependence of f_K/f_π, obtained using different definitions of the strange quark mass and tadpole improvement.

results show a puzzlingly-strong a dependence, which requires further investigation. So I cannot compare continuum extrapolations in the two improvement schemes.

Current normalisations cancel in the ratio f_K/f_π and the tadpole-improved data alone can be extrapolated reliably to the continuum limit. As shown in Fig 11, we find a significant disagreement between the quenched QCD estimate and experiment, and that, within our statistics, the continuum limit for this quantity is independent of the definition of the strange quark mass.

CONCLUSION

There is a striking level of agreement between the continuum extrapolations of the light-hadron spectrum obtained from non-perturbative $O(a)$ improvement and from tadpole improvement. Our continuum estimates have been obtained at fixed physical volume, corresponding to a linear size of about 1.7 fm. The smallness of this volume is a cause for concern, but our checks of finite-size effects, particularly for baryons, which are expected to be the worst affected, indicate that there is no significant effect.

Although there are differences at fixed lattice spacing, we obtain compatible continuum estimates for f_K, M_{K^*} and/or M_K, using different definitions of the strange quark mass, ie, from M_K, M_{K^*} and M_ϕ. Equivalently, we obtain consistent continuum estimates for the strange quark mass, in agreement with world data and at the low end of the range expected phenomenologically. It will be interesting to see if this low value turns out to be a quenching effect.

It appears, therefore, that QQCD works better as an effective theory in the continuum limit than it does at a fixed, non-zero lattice spacing. However, for some quantities in the light-hadron sector, such as M_N/M_ρ and f_K/f_π, the evidence is growing that the continuum limit of QQCD disagrees significantly with experiment. Thus, despite considerable success as an effective theory, numerical simulations are now becoming sufficiently precise to expose the limitations of the quenched approximation.

This progress has been due to a 10^5-fold increase in computer speed, to the development of more efficient and robust linear equation solvers, and to the implementation of the Symanzik improvement scheme to $O(a)$. Since 1981, lattice volumes have increased by 5^4, but the lattice spacing is almost unchanged! This last fact is strong encouragement for applying the improvement programme in simulations of QCD with dynamical quarks, where the computational cost is a much higher power of the number of lattice sites and finite-size effects are probably bigger.

Acknowledgements

This work supported by PPARC Grants GR/J98202, GR/K54601 and GR/K55745, by EPSRC Grant GR/K41663, and by EU Network Grant CHRX-CT92-0051. Figures 3 (left) and 5 are reprinted from references 12 and 32, respectively, with kind permission of Elsevier Science - NL, Sara Burgerhartstraat 25, 1055 KV Amsterdam, The Netherlands.

REFERENCES

1. H. Hamber and G. Parisi, *Phys. Rev. Lett.* 47 (1981) 1792.
2. F. Butler, H. Chen, A. Vaccarino and D. Weingarten, *Phys. Rev. Lett.* 70 (1993) 2849; *Nucl. Phys.* B421 (1994) 217; B430 (1994) 179.
3. R.D. Kenway (UKQCD Collaboration), Improvement and the continuum limit for quenched light hadrons, *in* Proceedings of the International Workshop "Lattice QCD on Parallel Computers", ed. Y. Iwasaki and A. Ukawa, *Nucl. Phys. B (Proc. Suppl.)* (1997) in press.
4. T. Yoshié (CP-PACS Collaboration), CP-PACS results with the Wilson action, *in* Proceedings of the International Workshop "Lattice QCD on Parallel Computers", ed. Y. Iwasaki and A. Ukawa, *Nucl. Phys. B (Proc. Suppl.)* (1997) in press.
5. I. Montvay and G. Münster, "Quantum Fields on a Lattice", Cambridge University Press, Cambridge (1994).
6. K.G. Wilson, *Phys. Rev.* D10 (1974) 2445; *in* "New Phenomena in Subnuclear Physics", ed. A. Zichichi, Plenum Press, New York (1975).
7. H.B. Nielsen and M. Ninomiya, *Nucl. Phys.* B185 (1981) 20; *Nucl. Phys.* B193 (1981) 173.
8. T. Banks et al., *Phys. Rev.* D15 (1976) 1111.
9. L. Susskind, *Phys. Rev.* D16 (1977) 3031.
10. H.P. Shanahan et al. (UKQCD Collaboration), *Phys. Rev.* D55 (1997) 1548.
11. A. Frommer, *Nucl. Phys. B (Proc. Suppl.)* 53 (1997) 120.
12. K.C. Bowler, D.L. Chalmers, A. Kenway, R.D. Kenway, G.S. Pawley and D.J. Wallace, *Phys. Lett.* 162B (1985) 354.
13. S. Ono, *Phys. Rev.* D17 (1978) 888.
14. M. Lüscher, *Commun. Math. Phys.* 104 (1986) 117; 105 (1986) 153.
15. S. Gottlieb, *Nucl. Phys. B (Proc. Suppl.)* 53 (1997) 155.
16. K. Jansen, C. Liu, M. Lüscher, H. Simma, S. Sint, R. Sommer, P. Weisz and U. Wolff, *Phys. Lett.* B372 (1996) 275.
17. K. Symanzik, *in* "Mathematical Problems in Theoretical Physics", eds R. Schrader et al., *Lecture Notes in Physics*, Vol. 153 (Springer, New York, 1982); *Nucl. Phys.* B226 (1983) 187 and 205.
18. M. Lüscher et al. (Alpha Collaboration), *Nucl. Phys.* B478 (1996) 365.
19. P. Weisz, *these Proceedings*.
20. B. Sheikholeslami and R. Wohlert, *Nucl. Phys.* B259 (1985) 572.
21. G. Heatlie et al., *Nucl. Phys.* B352 (1991) 266.
22. M. Bochicchio, L. Maiani, G. Martinelli, G. Rossi and M. Testa *Nucl. Phys.* B262 (1985) 331.
23. G.P. Lepage and P.B. Mackenzie, *Phys. Rev.* D48 (1993) 2250.
24. R.D. Kenway (UKQCD Collaboration), *Nucl. Phys.* B (Proc. Suppl.) 53 (1997) 206.
25. P.A. Rowland, *Nucl. Phys. B (Proc. Suppl.)* 53 (1997) 308.
26. M. Lüscher et al. (Alpha Collaboration), DESY preprint 96-222, `hep-lat/9611015`.
27. M. Lüscher et al. (Alpha Collaboration), *Nucl. Phys.* B491 (1997) 323.
28. S. Sint and P. Weisz, FSU preprint FSU-SCRI-97-24, `hep-lat/9704001`.
29. J. Gasser and H. Leutwyler, *Phys. Rep.* C87 (1982) 108.

30. S. Aoki and A. Gocksch, *Phys. Rev.* D45 (1992) 3845.
31. C. Bernard and M. Golterman, *Phys. Rev.* D46 (1992) 853.
32. S.R. Sharpe, *Nucl. Phys.* B (Proc. Suppl.) 53 (1997) 181.
33. R.M. Barnett et al. (Particle Data Group), *Phys. Rev.* D54 (1996) 1.
34. J. Donoghue, B. Holstein and D. Wyler, *Phys. Rev. Lett.* 69 (1992) 3444.
35. R. Gupta and T. Bhattacharya, Los Alamos preprint LAUR-96-1840, `hep-lat/9605039`.
36. G. Martinelli and Y. Zhang, *Phys. Lett.* B123 (1983) 433.
37. M. Golterman and J. Smit, *Phys. Lett.* B140 (1984) 392.
38. C.R. Allton et al. (APE Collaboration), *Nucl. Phys.* B431 (1994) 667.
39. W. Bardeen et al., Fermilab preprint FERMILAB-PUB-97/121-T, `hep-lat/9705008`.